



# Nanoporous separator and low fuel concentration to minimize crossover in direct methanol laminar flow fuel cells

A.S. Hollinger<sup>a</sup>, R.J. Maloney<sup>b</sup>, R.S. Jayashree<sup>b,1</sup>, D. Natarajan<sup>c</sup>, L.J. Markoski<sup>c,\*</sup>, P.J.A. Kenis<sup>a,b,\*\*</sup>

<sup>a</sup> Department of Mechanical Science and Engineering, University of Illinois at Urbana-Champaign, 1206 Green Street, Urbana, IL 61801, USA

<sup>b</sup> Department of Chemical & Biomolecular Engineering, University of Illinois at Urbana-Champaign, 600 S. Mathews Avenue, Urbana, IL 61801, USA

<sup>c</sup> INI Power Systems, 175 Southport Drive, Suite 100, Morrisville, NC 27560, USA

## ARTICLE INFO

### Article history:

Received 9 November 2009

Received in revised form

13 December 2009

Accepted 14 December 2009

Available online 22 December 2009

### Keywords:

Laminar flow

Fuel cell

Multichannel

Methanol crossover

Separator

## ABSTRACT

Laminar flow fuel cells (LFFCs) overcome some key issues – most notably fuel crossover and water management – that typically hamper conventional polymer electrolyte-based fuel cells. Here we report two methods to further minimize fuel crossover in LFFCs: (i) reducing the cross-sectional area between the fuel and electrolyte streams, and (ii) reducing the driving force of fuel crossover, i.e. the fuel concentration gradient. First, we integrated a nanoporous tracketch separator at the interface of the fuel and electrolyte streams in a single-channel LFFC to dramatically reduce the cross-sectional area across which methanol can diffuse. Maximum power densities of 48 and 70 mW cm<sup>-2</sup> were obtained without and with a separator, respectively, when using 1 M methanol. This simple design improvement reduces losses at the cathode leading to better performance and enables thinner cells, which is attractive in portable applications. Second, we demonstrated a multichannel cell that utilizes low methanol concentrations (<300 mM) to reduce the driving force for methanol diffusion to the cathode. Using 125 mM methanol as the fuel, a maximum power density of 90 mW cm<sup>-2</sup> was obtained. This multichannel cell further simplifies the LFFC design (one stream only) and its operation, thereby extending its potential for commercial application.

© 2010 Elsevier B.V. All rights reserved.

## 1. Introduction

As next-generation portable electronics continue to require ever-increasing energy densities, microfuel cells have attracted significant interest as an alternative to conventional batteries [1–4]. Unlike batteries which carry a limited supply of fuel internally, microfuel cells consume fuel which is continuously replenished. Microfuel cells can be operated with a variety of fuels, including: hydrogen [5–8], methanol [8–11], and formic acid [12,13]. Compared to hydrogen and other gaseous fuels, liquid fuels are easier to store and transport, and have much higher energy densities per weight and volume. In particular, direct methanol fuel cells (DMFCs) have attracted much interest in portable applications due to the high energy density of methanol.

Although DMFCs offer a promising method of energy conversion, development of DMFCs has been hampered by issues related to the polymer electrolyte membrane (PEM) that separates the anodic and cathodic compartments. Water and/or thermal management is one such concern because Nafion, the most commonly used ionomeric material, must remain fully hydrated to facilitate proton transport, which limits stack and system operation to less than 100 °C. More significantly, the permeation of methanol through the Nafion membrane, i.e. methanol crossover, results in mixed potentials at the cathode, and consequently a dramatic decrease in cell performance [14–18].

A desire to help eliminate these membrane constraints led to the development of laminar flow-based fuel cells (LFFCs) [19–32]. By utilizing laminar flow on the microscale, the fuel and/or electrolyte (or oxidant) streams may be compartmentalized in a single microchannel or a series of parallel microchannels without the need for a physical barrier such as a Nafion membrane. Microfluidic streams flow directly over the catalytic region of an electrode without an intervening thick gas diffusion layer, thus achieving the minimum possible mass transport distance. The membrane-less LFFC design utilizes a continuously flowing electrolyte to (i) minimize dry-out and flooding issues at the electrodes, (ii) facilitate by-product removal (i.e. carbon dioxide, carbonates), and (iii) enable fuel and media flexibility. Much work has been done in this field by our group [19–25] and others [26–32]. A

\* Corresponding author at: INI Power Systems, 175 Southport Dr., Suite 100, Morrisville, NC 27560, United States. Tel.: +1 919 677 7112.

\*\* Corresponding author at: Department of Chemical & Biomolecular Engineering, University of Illinois, 600 S. Mathews Ave., Urbana, IL 61801, United States. Tel.: +1 217 265 0523.

E-mail addresses: [ljmarkoski@inipower.com](mailto:ljmarkoski@inipower.com) (L.J. Markoski), [kenis@illinois.edu](mailto:kenis@illinois.edu) (P.J.A. Kenis).

<sup>1</sup> Present address: Department of Chemistry, Georgia State University, P.O. Box 4098, Atlanta, GA 30302, USA.

recent review provides a thorough summary of the field of LFFCs [33].

In LFFC architectures presented to date, fuel crossover depends strongly on (i) cross-sectional area between the anode and cathode as well as (ii) the driving force, i.e. the concentration gradient. Here, we will present two approaches for reducing fuel crossover in LFFCs. At high concentrations of methanol (1–5 M), crossover can be mitigated by pressing the fuel concentration boundary close to the anode catalytic wall via high (differential) flow rates or by using wide channels. However, high flow rates reduce fuel utilization and wide channels increase electrode-to-electrode distances [34]. Our first, more effective approach to reduce fuel crossover involves placing a nanoporous separator at the fuel–electrolyte interface of an LFFC. This separator greatly minimizes the total cross-sectional area at the fuel–electrolyte interface, and hence, the area through which unreacted methanol molecules can crossover to the parallel-flowing electrolyte stream, and ultimately the cathode. This design improvement maintains small electrode-to-electrode distances for reduced volume and higher power density. Our second approach to reduce fuel crossover is to operate at low fuel concentrations, thereby decreasing the driving force for methanol crossover. In a methanol LFFC, crossover is limited to the slow process of diffusion, a concentration gradient-controlled phenomenon. By operating at low methanol concentrations (less than 100 mM), mixed potential effects are not observed when platinum is used as the cathode catalyst [24]. Below we will explore these two approaches using single and multichannel LFFCs.

## 2. Experimental

### 2.1. Single-channel methanol LFFC

#### 2.1.1. Fabrication and assembly

The 6- $\mu\text{m}$  thick polycarbonate separator (0.05- $\mu\text{m}$  pore size,  $6 \times 10^8$  pores  $\text{cm}^{-2}$ , Sterlitech Corporation) was placed between two identical 150- $\mu\text{m}$  thick Kapton sheets, which were machined to have 4.8 cm (L)  $\times$  0.33 cm (W) flow channels. The small characteristic height (defined by the Kapton thickness) of the channels lead

to low Reynolds numbers ( $\text{Re} < 5$ ), enabling the fuel and electrolyte streams to flow laminarily in parallel on either side of the separator. The anode was centered on a polymer-impregnated graphite plate (McMaster), which functions as a current collector. The cathodic gas diffusion electrode (GDE) was placed in a 220- $\mu\text{m}$  deep trench machined into a similar graphite plate. Within this trench, a serpentine flow channel was machined with a 1:1 channel to landing ratio, and channel dimensions of 1 mm (H)  $\times$  1 mm (W). This serpentine channel thus resides exactly beneath the cathodic GDE when it is placed in the trench. Two copper backing plates were placed on either side of the fuel cell to render a robust multilayer assembly as shown in Fig. 1a and b. A cartridge heater can be inserted into the copper plate on the anode side for studies at elevated temperatures. The entire apparatus was held together by 14 evenly spaced bolts, greatly reducing contact resistance between layers. This approach yields a leak-free cell; gaskets were not required.

#### 2.1.2. Electrode preparation

An anode catalyst ink comprised of 10 mg  $\text{cm}^{-2}$  Pt–Ru 50:50 wt% alloy (Alfa Aesar) with 125  $\mu\text{L}$   $\text{H}_2\text{O}$ , 34.5  $\mu\text{L}$  Nafion solution, and 125  $\mu\text{L}$  isopropyl alcohol, and a cathode catalyst ink comprised of 2 mg  $\text{cm}^{-2}$  Pt–C 50:50 atom wt% alloy (Alfa Aesar) with 31.25  $\mu\text{L}$   $\text{H}_2\text{O}$ , 1.15  $\mu\text{L}$  Nafion, and 31.25  $\mu\text{L}$  isopropyl alcohol were used for all experiments reported here. The catalyst inks were sonicated (Branson 3510) for 1 h to obtain a uniform mixture, before being brushed onto Sigracet 35BC carbon paper. Similar to prior work [35,36], both electrodes were then hot-pressed (Carver Laboratory Press) at 1200 psi for 5 min at 130  $^\circ\text{C}$  to improve catalyst adhesion and electrode durability. For some experiments, an additional layer of Nafion 212 (Fuel Cell Scientific, Stoneham, MA), cleaned in a solution of 10 wt% nitric acid at 90  $^\circ\text{C}$  for 2 h, was bonded to the cathodic GDE, during the hot-pressing procedure.

#### 2.1.3. Testing

Unless otherwise noted, the single-channel methanol LFFC was operated at 80  $^\circ\text{C}$ , with an  $\text{O}_2$  supply (laboratory grade, S.J. Smith) of 50 sccm to the serpentine flow field, a fuel and electrolyte flow rate of 0.3  $\text{mL min}^{-1}$ , a fuel stream of 1 M methanol with 1 M

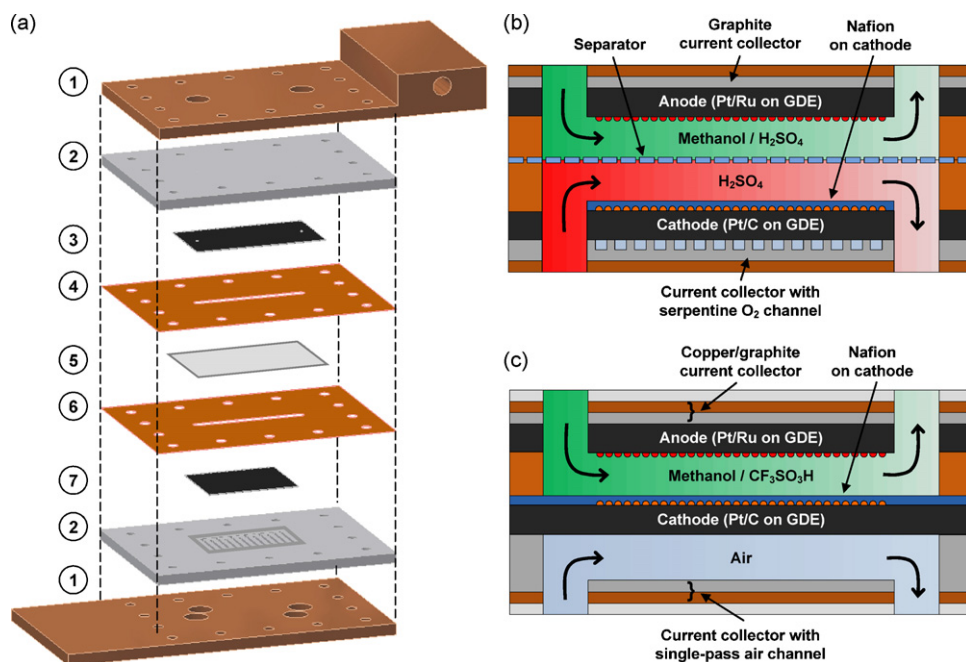


**Fig. 1.** (a) Exploded diagram of single-channel methanol LFFC (to scale), the numbered components correspond to: (1) copper backing plate with temperature control, (2) graphite current collector, (3) anode, (4) fuel channel, (5) separator, (6) electrolyte channel, and (7) cathode; (b) side-view schematic of single-channel methanol LFFC (exactly like (a)); (c) side-view schematic of multichannel methanol LFFC.

H<sub>2</sub>SO<sub>4</sub> added for proton conduction, and an electrolyte stream of 1 M H<sub>2</sub>SO<sub>4</sub>. The fuel and electrolyte streams were driven through polyethylene tubing (Intramedic, ID = 1.14 mm) and into the cell using a syringe pump (Harvard Instruments). Fuel cell testing was conducted using a potentiostat (Autolab PGSTA-30, Eco Chemie B.V.) and polarization curves were obtained by measuring the current at different set cell potentials after steady state was reached. An Ag/AgCl reference electrode (saturated NaCl, BAS, West Lafayette, IN) was placed at the outlet of the electrolyte stream to enable the independent analysis of polarization losses of the anode and cathode [21].

## 2.2. Multichannel methanol LFFC

### 2.2.1. Fabrication and assembly

In the multichannel cell, methanol in dilute concentrations (and 250 mM trifluoromethanesulfonic acid) was driven through a 1 mm thick graphite inlet manifold which distributed the fuel to 14 parallel microfluidic flow channels. The 14 mm (L) × 2 mm (W) channels were machined into a 75- $\mu$ m thick Kapton sheet. The exiting fuel was connected to another 1 mm thick graphite outlet manifold to complete the fluid path. The anode and cathode were centered between the two graphite plates, which also served as current collectors. Beneath the cathodic GDE, a serpentine single-pass gas channel with dimensions of 0.75 mm (H) × 1 mm (W) was machined into the graphite plate. The gas channel is positioned such that the individual windings are arranged parallel to the microfluidic channels. Copper plates were placed on either side of the graphite plates for increased current collection. A Kapton tape heater was included in this assembly to enable studies at elevated temperatures. The entire assembly was loaded to 400 lbs in a hydraulic press (Carver Laboratory Press) and bolted together between two aluminum end-plates to yield a multichannel methanol LFFC as depicted in Fig. 1c.

### 2.2.2. Electrode preparation

An anode catalyst ink comprised of 6.45 mg cm<sup>-2</sup> Pt–Ru 50:50 atom wt% alloy (Johnson–Matthey), and a cathode catalyst ink comprised of 1.75 mg cm<sup>-2</sup> Pt–C 50:50 atom wt% alloy (Johnson–Matthey) were used for all experiments reported here. The anode catalyst had a metal to Nafion ratio of 9:1 by weight while the supported catalyst to Nafion weight ratio in the cathode catalyst was 2:1. The catalyst inks were sonicated for 30 min and stirred for 30 min to obtain a uniform mixture. The anode ink was brushed onto Toray carbon paper TGPH-30 and the cathode ink was brushed onto Sigracet 24BC carbon paper. Both electrodes were hot-pressed at 725 psi for 7 min at 135 °C to improve catalyst adhesion and electrode durability. An additional layer of Nafion 212 (Ion Power Inc.) was bonded to the cathodic GDE during the hot-pressing procedure. A photo-etched Kapton layer (leaving the cathode exposed) was then bonded at the above-mentioned conditions on top of the Nafion layer for mechanical stability. The fuel and electrolyte flow in the Kapton channel layer directly over the anode catalyst layer and the photo-etched Kapton layer, making this multichannel cell a single-stream version of the dual-stream, single-channel cell described above (Section 2.1).

### 2.2.3. Testing

Unless otherwise noted, the multichannel methanol LFFC was operated at 70 °C, with high purity air from a compressed gas cylinder at a stoichiometric flow ratio (stoic) of at least 3 at any given current, and an electrolyte stream of 0.25 M trifluoromethanesulfonic acid (CF<sub>3</sub>SO<sub>3</sub>H). Fuel concentration was varied from 0.063 to 0.25 M methanol. A fluid pump (Encynova) with digital control was used for recirculation of the liquid stream. Before testing, the cell heater was set to 70 °C, the 0.25 M trifluoromethanesulfonic acid

was pre-heated to 70 °C and circulated through the cell until thermal equilibrium was attained. Due to heat losses in the fluid lines and pump, the exit temperature of the liquid was 60–65 °C depending on flow rates. The circulating fluid volume was chosen to be 1 L to avoid significant fuel concentration changes over the course of the experiment. Pure methanol was added to the circulating stream to provide the desired fuel concentration.

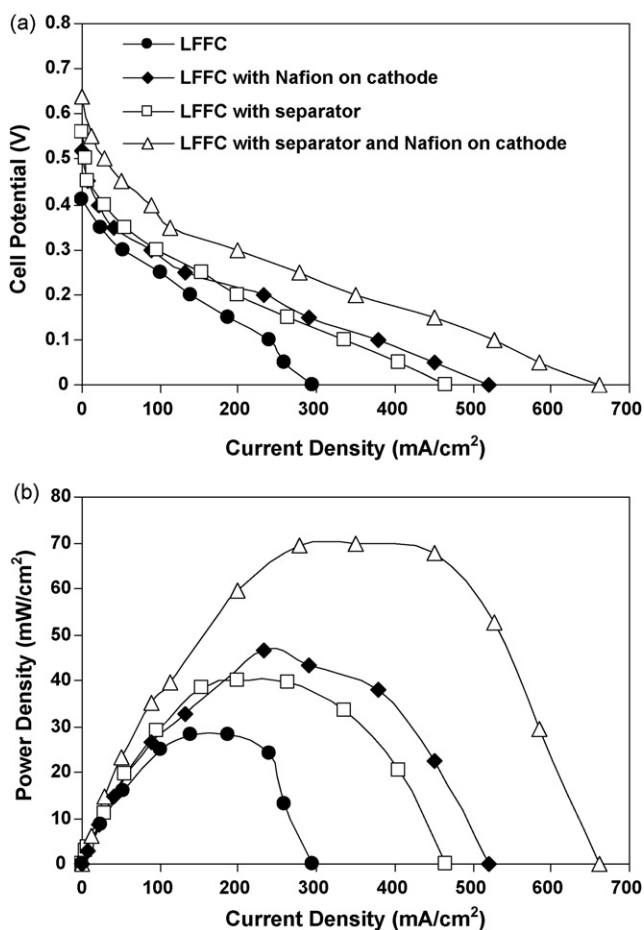
Before testing, the cell was discharged galvanostatically using one of the channels in an 8-channel Solartron 1470E multi-stat. The cell was held at each current for 90 s. A frequency response analyzer, Solartron 1252 A was used to conduct a frequency sweep at a magnitude of 10 mA at each galvanic step. The real axis intercept of the frequency scan was used to estimate the ohmic (i.e. IR) drop. A sufficient number of preliminary galvanostatic scans were conducted to stabilize and condition the cell and to ensure reproducibility before final polarization measurements were obtained. The voltage response at each current step was averaged over the last 30 s to obtain polarization curves. A condenser eliminated water vapor from the air exit stream, which was then diluted with nitrogen to allow the use of a CO<sub>2</sub> analyzer for crossover measurement. Methanol crossover rates were calculated based on the CO<sub>2</sub> concentration in the air exit stream, measured at select current steps.

## 3. Results and discussion

### 3.1. Performance of a single-channel methanol LFFC with a separator

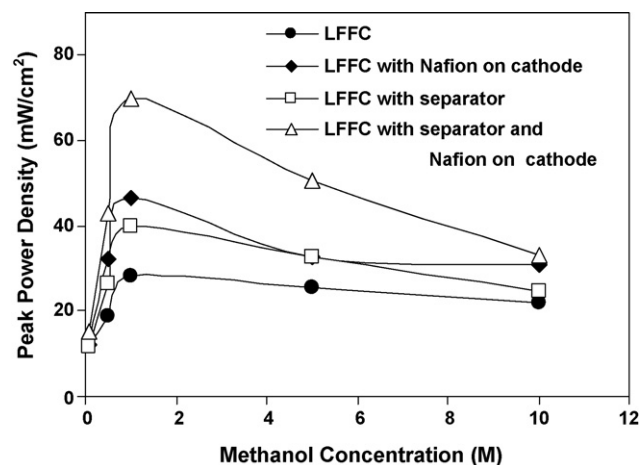
In an effort to reduce methanol crossover, while still maintaining small electrode-to-electrode distances, a thin polycarbonate separator was placed between the fuel and electrolyte streams of a single-channel methanol LFFC. This nanoporous polymer (0.05- $\mu$ m pore size,  $6 \times 10^8$  pores cm<sup>-2</sup>) functions to reduce the liquid–liquid contact between these two streams by 98.8%. Greatly reducing the interfacial contact between the fuel and electrolyte streams limits the regions where unreacted molecules of methanol can diffuse toward the cathode. Thus, initially unreacted molecules of methanol are more likely to either react farther downstream in the fuel channel or be swept out with the fuel stream, than to crossover to the electrolyte stream or the cathode. The separator is not selective to methanol and hence may also limit proton diffusion to the cathode. However, the diffusion coefficient of protons in aqueous media is approximately one order of magnitude larger than the diffusion coefficient of methanol in aqueous media ( $D_{H^+(water)} = 9.31 \times 10^{-5}$  cm<sup>2</sup> s<sup>-1</sup> vs.  $D_{MeOH(water)} = 1.58 \times 10^{-5}$  cm<sup>2</sup> s<sup>-1</sup> [37]). In addition, proton transport rates are augmented by the potential gradient between the electrodes, while methanol transport is dominated by diffusion. Consequently, the separator has a greater impact on the slower methanol transport processes than the rapid proton transport processes. A thin Nafion 212 layer was hot-pressed to the cathodic GDE as an additional barrier to methanol crossover [35]. This layer of Nafion functions to further slow methanol molecules from diffusing to the cathode catalyst, as the diffusion coefficient of methanol in Nafion is approximately one order of magnitude smaller than the diffusion coefficient of methanol in water ( $D_{MeOH(Nafion)} = 3.0 \times 10^{-6}$  cm<sup>2</sup> s<sup>-1</sup> vs.  $D_{MeOH(water)} = 1.58 \times 10^{-5}$  cm<sup>2</sup> s<sup>-1</sup> [38]).

Fig. 2 shows the polarization and power density curves for a single-channel methanol LFFC operated with and without a separator and, with and without Nafion on the cathode. A maximum open circuit potential (OCP) of 0.64 V was obtained when operating with the separator in place and with Nafion on the cathode. The OCP gradual decreases when there is no Nafion (0.56 V), no separator (0.5 V), and neither a separator or Nafion (0.41 V). This can be attributed to an increase in methanol crossover. The power density



**Fig. 2.** (a) Polarization and (b) power density curves of a single-channel methanol LFFC operating at 80 °C with 1 M methanol, an O<sub>2</sub> supply of 50 sccm, a fuel and electrolyte flow rate of 0.3 mL min<sup>-1</sup>, two different cathode preparations (with and without hot-pressing Nafion), and with or without a separator.

curves show that an LFFC operated without a separator or Nafion on the cathode produces a maximum power density of 28 mW cm<sup>-2</sup>. Adding either a separator or Nafion to the cathode, increases the maximum power density to more than 40 mW cm<sup>-2</sup>. By adding



**Fig. 3.** Peak power density of a single-channel methanol LFFC operating at 80 °C, an O<sub>2</sub> supply of 50 sccm, a fuel and electrolyte flow rate of 0.3 mL min<sup>-1</sup>, two different cathode preparations (with and without hot-pressing of Nafion on the cathode), and with or without a separator, for a range of methanol concentrations. Lines through the data points are added to guide the eye.

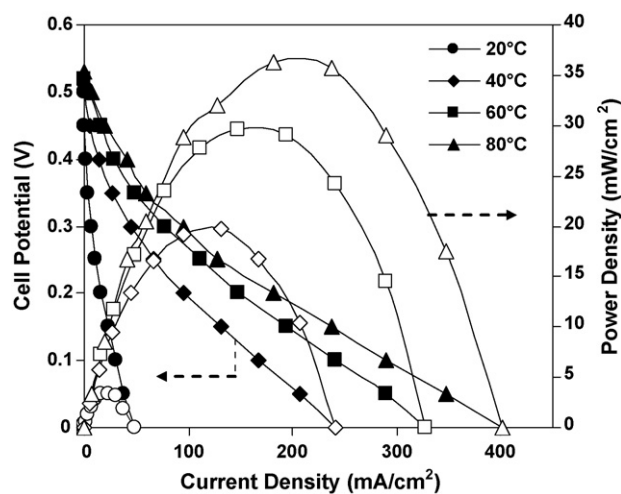


**Fig. 4.** Polarization (closed data points) and power density (open data points) curves of a single-channel methanol LFFC operating with a separator and with Nafion on cathode, with 1 M methanol, an O<sub>2</sub> supply of 50 sccm, and a fuel and electrolyte flow rate of 0.3 mL min<sup>-1</sup> for a range of temperatures. The cathode and anode electrodes used in this LFFC were not optimized for best performance.

both, the maximum power density increases to 70 mW cm<sup>-2</sup>. This increase in maximum power density shows that the result of adding a separator and the result of adding Nafion to the cathode are additive.

### 3.1.1. The effect of concentration and temperature

Irrespective of Nafion or the separator being implemented, a methanol concentration of 1 M led to maximum power densities for this single-channel cell (Fig. 3). At lower methanol concentrations (100–500 mM), fuel concentration polarization losses at the anode is the performance-limiting factor, while at higher concentrations (5–10 M), the decrease in power density can be attributed to increased crossover. Fig. 3 also indicates that the power density increased comparably when a separator was added to a methanol LFFC that operates at higher concentrations of methanol. At a methanol concentration of 1 M, the power density increased by 43%, from 28 to 40 mW cm<sup>-2</sup>, when a separator was added to an LFFC that did not have Nafion on the cathode. The power density increased by 51%, from 48 to 70 mW cm<sup>-2</sup>, when a separator was

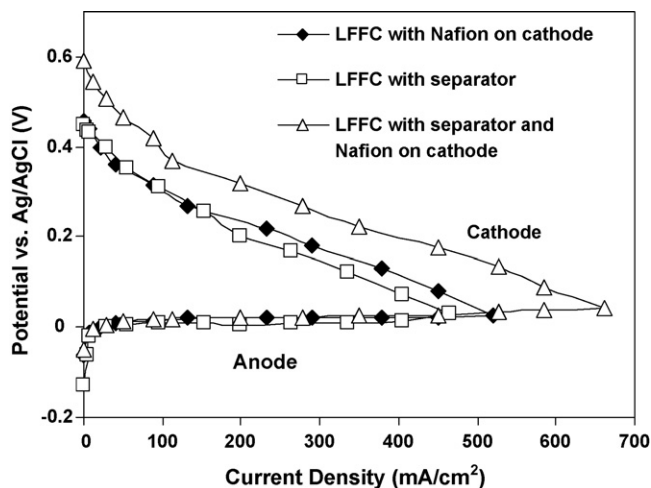


**Fig. 5.** Anode and cathode potentials vs. Ag/AgCl of a single-channel methanol LFFC operating at 80 °C with 1 M methanol, an O<sub>2</sub> supply of 50 sccm, a fuel and electrolyte flow rate of 0.3 mL min<sup>-1</sup>, two different cathode preparations (with and without hot-pressing Nafion), and with or without a separator.

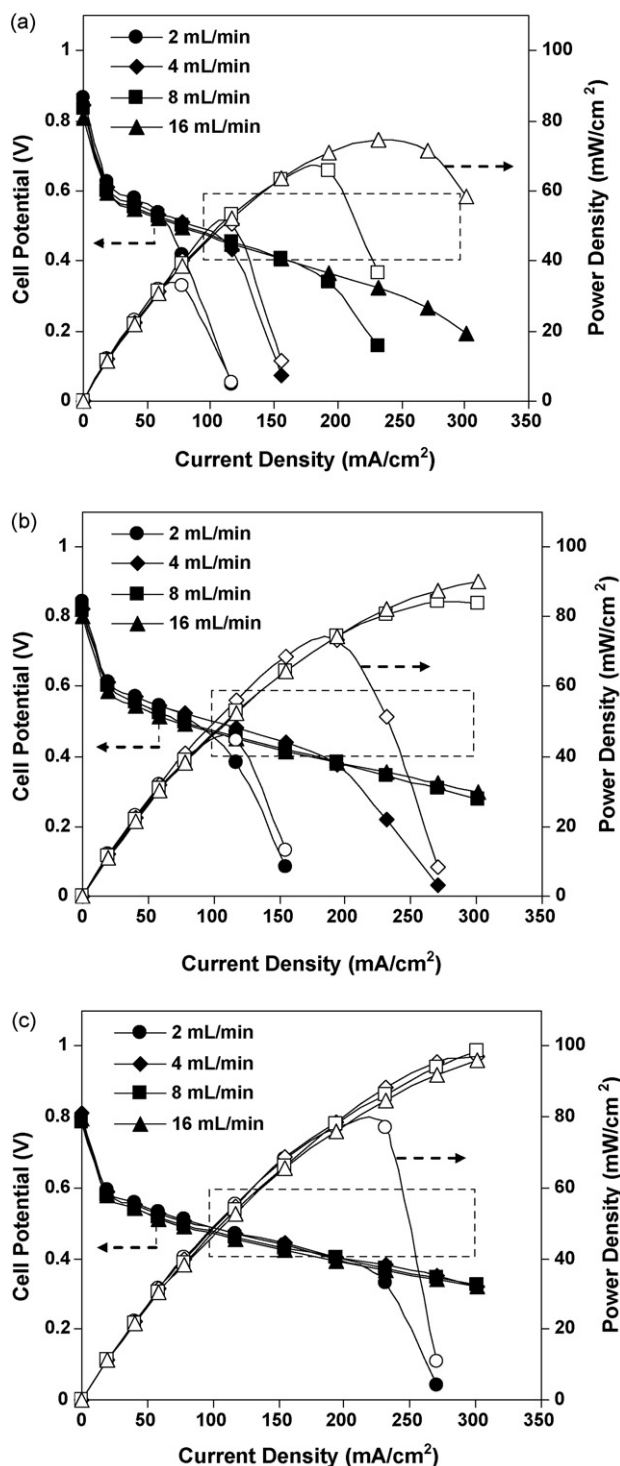


**Fig. 6.** Polarization and power density curves of multichannel LFFC operating at 70 °C with (a) 0.063 M methanol, (b) 0.125 M methanol, and (c) 0.25 M methanol in 0.25 M triflic acid for a range of flow rates. The dashed box represents a commercially desirable performance window.

added to an LFFC that had Nafion on the cathode. The comparable improvement in power densities indicates that implementing a separator improves LFFC performance irrespective of Nafion being used on the cathode.

Fig. 4 compares the polarization and power density curves of a single-channel methanol LFFC with separator and Nafion on the cathode, operating at different temperatures. Despite the implementation of the separator and the Nafion layer on the cathode, this

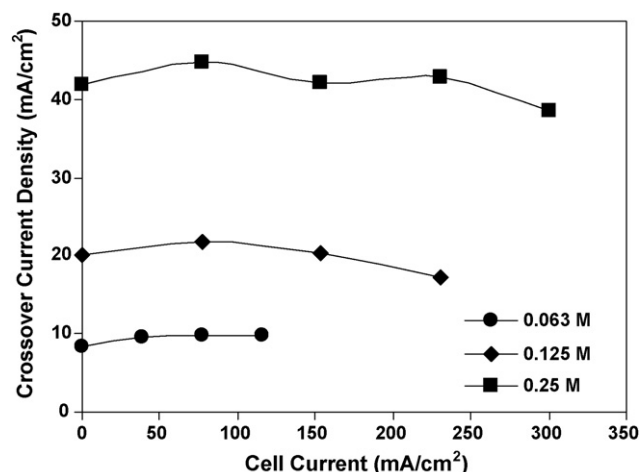


**Fig. 7.** Methanol crossover in a multichannel LFFC, without nanoporous separator, as a function of cell current for three different methanol concentrations (uncorrected for CO<sub>2</sub> crossover from the anode stream). The cell is operated at 70 °C, with a fuel flow rate of 8 mL min<sup>-1</sup>, and constant air stoic of 3.

LFFC exhibits the expected increase in performance with increasing temperature, as observed in other reported DMFCs [39].

### 3.1.2. Relative performance of individual electrodes

Polarization curves of the individual electrodes obtained by using a Ag/AgCl reference electrode show that the cathode suffers significantly more polarization losses than the anode (Fig. 5). Highest current densities are observed with a separator and with Nafion on the cathode. This reveals that the enhanced performance stems from the separator and the Nafion layer on the cathode. These two additional elements further reduce fuel crossover leading to smaller polarization losses on the cathode. Results from the LFFC operated without a separator and without a Nafion layer on the cathode are not reported in Fig. 5 because CO<sub>2</sub> bubbles that form on the anode crossed into the electrolyte stream, thereby intermittently breaking the electrical contact to the reference electrode.

### 3.2. Performance of a multichannel methanol LFFC with low fuel concentrations

In a second effort to reduce methanol crossover, a multichannel LFFC was operated at low fuel concentrations. A challenge will be to do this while avoiding polarization losses at the anode due to the lower fuel concentration. A key potential benefit of using low fuel concentrations in an LFFC is that it could result in an increase in overall fuel utilization. Fig. 6 shows the polarization and power density curves for a multichannel methanol LFFC at three different methanol concentrations and four different flow rates. Performance is a strong function of flow rate at lower methanol concentrations but becomes a weaker function at higher concentrations. OCPs ranged from 0.87 to 0.81 V over the range of methanol concentrations used (0.063, 0.125, and 0.25 M). The gradual decrease in the OCP is a result of increased methanol crossover at higher fuel concentrations.

We calculated a commercially desirable operating window based on the highest power density that can be achieved while maintaining catalyst durability for 2000–3000 operating hours with less than 20% performance degradation. The performance of the multichannel LFFC, as shown in Fig. 6, fell within the commercially desirable operating window for all but one of the operating conditions tested namely very low flow rate (0.2 mL min<sup>-1</sup>) and low concentration (0.063 M).

### 3.2.1. Methanol crossover measurements

Methanol crossover measurements were calculated based on the CO<sub>2</sub> concentration in the exiting air stream of the multichannel methanol LFFC. Recall that this cell does not have a nanoporous separator. In this experiment, the fuel flow rate is held constant at 8 mL min<sup>-1</sup>. Since the crossover rate to the cathode is a diffusion-controlled process, an increase in flow rate is not expected to have a significant impact on the crossover rate. The data in Fig. 7 confirms that crossover rates increase at higher methanol concentrations in a multichannel methanol LFFC. More specifically, the crossover rate is shown to increase linearly with increases in methanol concentration, reaching ~40 mA cm<sup>-2</sup> at a methanol concentration of 0.25 M. This data was not corrected for CO<sub>2</sub> crossover and hence the extent of crossover during cell discharge may be overestimated slightly [40].

## 4. Conclusions

Laminar flow-based fuel cells (LFFCs) have been developed to help eliminate the common membrane selectivity issues in polymer electrolyte fuel cells, however fuel crossover is still present in LFFCs and it is strongly dependent upon the LFFC's cross-sectional area, the electrode-to-electrode distance, as well as the fuel concentration gradient between the anode and cathode. Here we present two ways to mitigate fuel crossover by reducing bulk mass transport (and not by improving selective species transport): (i) using a nanoporous separator between anode and electrolyte stream, thereby minimizing the cross-sectional area across which methanol can diffuse; and (ii) using low methanol concentrations, thereby reducing the driving force for methanol diffusion. Together, these approaches present a scheme for operating over a wide range of methanol concentrations. The addition of a separator is a simple design change that maintains small electrode-to-electrode distances, making thinner methanol LFFCs possible that can be operated at higher methanol concentrations (~1 M). Operation at lower methanol concentrations (<300 mM) further simplified the multichannel cell's design, and is expected to result in higher overall fuel utilization. Performance of this cell falls in a window that is desirable for commercial application.

## Acknowledgements

This work was supported through an STTR Phase II grant from ARO to INI Power Systems of Morrisville, NC and the University of Illinois at Urbana-Champaign (W911NF-04-C-113). Financial support from the University of Illinois, from the National Science Foundation for a CAREER award to PJAK (NSF CTS 05-47617), and from the US Army Core of Engineers' Construction Engineering Research Laboratory (USACE-CERL) for a fellowship to ASH are also gratefully acknowledged. The authors thank Fikile Brushett for stimulating discussions.

## References

[1] C.K. Dyer, Fuel Cells Bulletin 2002 (2002) 8–9.

- [2] A. Heinzl, C. Hebling, M. Muller, M. Zedda, C. Muller, Journal of Power Sources 105 (2002) 250–255.
- [3] C. Cremers, M. Scholz, W. Seliger, A. Racz, W. Knechtel, J. Rittmayr, F. Grafwallner, H. Peller, U. Stimming, Fuel Cells 7 (2007) 21–31.
- [4] A. Kundu, J.H. Jang, J.H. Gil, C.R. Jung, H.R. Lee, S.H. Kim, B. Ku, Y.S. Oh, Journal of Power Sources 170 (2007) 67–78.
- [5] J.D. Morse, A.F. Jankowski, R.T. Graff, J.P. Hayes, Journal of Vacuum Science and Technology A: Vacuum Surfaces and Films 18 (2000) 2003–2005.
- [6] K. Shah, W.C. Shin, R.S. Besser, Sensors and Actuators B: Chemical 97 (2004) 157–167.
- [7] S.-S. Hsieh, C.-F. Huang, J.-K. Kuo, H.-H. Tsai, S.-H. Yang, Journal of Solid State Electrochemistry 9 (2005) 121–131.
- [8] C. Appleby, D. Ingersoll, P. Atanassov, D. Maricle, S. Sarangapani, Journal of Power Sources 162 (2006) 255–261.
- [9] J. Li, C. Moore, P.A. Kohl, Journal of Power Sources 138 (2004) 211–215.
- [10] S. Motokawa, M. Mohamedi, T. Momma, S. Shoji, T. Osaka, Electrochemistry 73 (2005) 346–351.
- [11] K. Wozniak, D. Johansson, M. Bring, A. Sanz-Velasco, P. Enoksson, Journal of Micromechanics and Microengineering 14 (2004) S59–S63.
- [12] C. Rice, S. Ha, R.I. Masel, P. Waszczuk, A. Wieckowski, T. Barnard, Journal of Power Sources 111 (2002) 83–89.
- [13] J. Yeom, R.S. Jayashree, C. Rastogi, M.A. Shannon, P.J.A. Kenis, Journal of Power Sources 160 (2006) 1058–1064.
- [14] D. Chu, S. Gilman, Journal of the Electrochemical Society 141 (1994) 1770–1773.
- [15] P.S. Kauranen, E. Skou, J. Munk, Journal of Electroanalytical Chemistry 404 (1996) 1–13.
- [16] K. Scott, W.M. Taama, P. Argyropoulos, K. Sundmacher, Journal of Power Sources 83 (1999) 204–216.
- [17] A. Heinzl, V.M. Barragan, Journal of Power Sources 84 (1999) 70–74.
- [18] V.A. Paganin, E. Sitta, T. Iwasita, W. Vielstich, Journal of Applied Electrochemistry 35 (2005) 1239–1243.
- [19] E.R. Choban, L.J. Markoski, A. Wieckowski, P.J.A. Kenis, Journal of Power Sources 128 (2004) 54–60.
- [20] E.R. Choban, J.S. Spendelov, L. Gancs, A. Wieckowski, P.J.A. Kenis, Electrochimica Acta 50 (2005) 5390–5398.
- [21] E.R. Choban, P. Waszczuk, P.J.A. Kenis, Electrochemical and Solid-State Letters 8 (2005) A348–A352.
- [22] R.S. Jayashree, L. Gancs, E.R. Choban, A. Primak, D. Natarajan, L.J. Markoski, P.J.A. Kenis, Journal of the American Chemical Society 127 (2005) 16758–16759.
- [23] R.S. Jayashree, D. Egas, J.S. Spendelov, D. Natarajan, L.J. Markoski, P.J.A. Kenis, Electrochemical and Solid-State Letters 9 (2006) A252–A256.
- [24] D.T. Whipple, R.S. Jayashree, D. Egas, N. Alonso-Vante, P.J.A. Kenis, Electrochimica Acta 54 (2009) 4384–4388.
- [25] F.R. Brushett, R.S. Jayashree, W.-P. Zhou, P.J.A. Kenis, Electrochimica Acta 54 (2009) 7099–7105.
- [26] S.M. Mitrovski, L.C.C. Elliott, R.G. Nuzzo, Langmuir 20 (2004) 6974–6976.
- [27] A. Bazylak, D. Sinton, N. Djilali, Journal of Power Sources 143 (2005) 57–66.
- [28] J.L. Cohen, D.J. Volpe, D.A. Westly, A. Pechenik, H.D. Abruna, Langmuir 21 (2005) 3544–3550.
- [29] E. Kjeang, A.G. Brolo, D.A. Harrington, N. Djilali, D. Sinton, Journal of the Electrochemical Society 154 (2007) B1220–B1226.
- [30] M.H. Sun, G. Velve Casquillas, S.S. Guo, J. Shi, H. Ji, Q. Ouyang, Y. Chen, Microelectronic Engineering 84 (2007) 1182–1185.
- [31] D.H. Ahmed, H.B. Park, H.J. Sung, Journal of Power Sources 185 (2008) 143–152.
- [32] E. Kjeang, R. Michel, D.A. Harrington, D. Sinton, N. Djilali, Electrochimica Acta 54 (2008) 698–705.
- [33] E. Kjeang, N. Djilali, D. Sinton, Journal of Power Sources 186 (2009) 353–369.
- [34] R.S. Jayashree, S.K. Yoon, F.R. Brushett, D. Natarajan, L.J. Markoski, P.J.A. Kenis, Journal of Power Sources 195 (2010) 3569–3578.
- [35] I.D. Raistrick, "Electrode Assembly for Use in a Solid Polymer Electrolyte Fuel Cell", United States, 1989.
- [36] E.A. Ticianelli, C.R. Derouin, A. Redondo, S. Srinivasan, Journal of the Electrochemical Society 135 (1988) 2209–2214.
- [37] P. Atkins, J.D. Paula, Atkins' Physical Chemistry, Oxford University Press, New York, 2002, p. 1104.
- [38] H.A. Every, M.A. Hickner, J.E. McGrath, T.A. Zawodzinski, Journal of Membrane Science 250 (2005) 183–188.
- [39] J. Nordlund, G. Lindbergh, Journal of the Electrochemical Society 151 (2004) A1357–A1362.
- [40] R. Jiang, D. Chu, Electrochemical and Solid-State Letters 5 (2002) A156–A159.